Folding in the Skyrme Model

Conor J. Houghton*

School of Mathematics
Trinity College, Dublin 2
Ireland

and Steffen Krusch†

Department of Applied Mathematics and Theoretical Physics
Centre for Mathematical Sciences, Wilberforce Road, Cambridge CB3 0WA
England

April 2001

Abstract

There are only three stable singularities of a differentiable map between three-dimensional manifolds, namely folds, cusps and swallowtails. A Skyrme configuration is a map from space to SU_2, and its singularities correspond to the points where the baryon density vanishes. In this paper we consider the singularity structure of Skyrme configurations.

The Skyrme model can only be solved numerically. However, there are good analytic ansätze. The simplest of these, the rational map ansatz, has a non-generic singularity structure. This leads us to introduce a non-holomorphic ansatz as a generalization. For baryon number two, three and four, the approximate solutions derived from this ansatz are closer in energy to the true solutions than any other ansatz solution. We find that there is a tiny amount of negative baryon density for baryon number three, but none for two or four. We comment briefly on the relationship to Bogomolny-Prasad-Sommerfield monopoles.

*houghton@maths.tcd.ie
†s.krusch@damtp.cam.ac.uk

1 Introduction

The Skyrme model is a nonlinear SU_2 field theory [1]. In addition to the fundamental excitations, the spectrum also includes topologically-charged soliton solutions. The model was proposed by Skyrme as a theory of nuclear physics in which the fundamental excitations are pions and the solitons are nucleons. The Skyrme energy function is

$$E = \int \left\{ -\frac{1}{2}\mathrm{Tr}\,(R_i R_i) - \frac{1}{16}\mathrm{Tr}([R_i, R_j][R_i, R_j]) \right\} \mathrm{d}^3x, \tag{1}$$

where R_i is the su_2-valued current $R_i = (\partial_i U)U^{-1}$. The SU_2-valued field U is required to attain its vacuum value, the identity, at spatial infinity and, so, it is a map between topological three-spheres. This is the origin of the topological charge, B.

The 1-Skyrmion is spherical and is given by the hedgehog ansatz

$$U_1(\mathbf{x}) = \exp(if(r)\ \widehat{\mathbf{n}} \cdot \boldsymbol{\sigma}), \tag{2}$$

where $\widehat{\mathbf{n}} = \widehat{\mathbf{x}}$ is the outward pointing unit normal and $\boldsymbol{\sigma} = (\sigma_1, \sigma_2, \sigma_3)$ are the Pauli matrices. $f(r)$ is a shape function and is usually determined numerically. It is very well approximated by the kink profile [2]: $f(r) = 4\arctan(\exp(-r))$. The 1-Skyrmion has six zero modes: three translational modes and three isospin modes corresponding to global SU_2 transformations.

Two well-separated Skyrmions attract or repel, depending upon their mutual isospin orientation. Two attracting 1-Skyrmions will move towards each other and form a bound state whose energy is 0.95 times the energy of two 1-Skyrmions. This 2-Skyrmion is torus shaped [3, 4] and is axially symmetric, in the sense that axial rotations in space are equivalent to isospin rotations, which are conjugations of U by a constant SU_2 matrix.

In the Skyrme model, the classical B-nucleon nucleus is a B-Skyrmion; that is, a minimum energy Skyrme field with topological charge B. For B from three to 22, the Skyrmion has been calculated numerically by evolving an attractive configuration, [5, 6, 7]. All the known Skyrmions have the bulk of their energy density on a fullerene-like shell. A geometric interpretation of this shell-like structure was given in [8]. Furthermore, Skyrmions often have a very symmetrical shape.

1.1 The Rational Map Ansatz

The rational map ansatz introduced in [9] is a simple ansatz for Skyrmions. It is similar to the 1-Skyrmion (2). The 1-Skyrmion is a hedgehog map in which the outward pointing unit normal, $\widehat{\mathbf{n}}$, maps a two-sphere identically to a two-sphere. In the ansatz, the hedgehog map is replaced by a more general holomorphic map, $\widehat{\mathbf{n}}_R$, from Riemann sphere to Riemann sphere. The rational map ansatz is given by

$$U(r, z) = \exp(if(r)\ \widehat{\mathbf{n}}_R \cdot \boldsymbol{\sigma}), \tag{3}$$

where

$$\widehat{\mathbf{n}}_R = \frac{1}{1 + |R|^2}(2\mathrm{Re}(R), 2\mathrm{Im}(R), 1 - |R|^2) \tag{4}$$

and $R(z)$ is a holomorphic map in z. Here, z is related to the standard angular coordinates ϕ and θ by the stereographic projection $z = \tan(\theta/2)\exp(i\phi)$. R is also a stereographic

coordinate on the Riemann sphere. In the ansatz, this Riemann sphere is a latitudinal two-sphere in $\mathrm{SU}_2 \cong S^3$.

The ansatz maps spheres around the origin in space to latitudinal two-spheres in SU_2. The shape function f is a function of r only, so each map between two-spheres is identical. The boundary conditions on f are $f(0) = \pi$ and $f(\infty) = 0$. These conditions are determined by requiring that U is well defined at the origin and attains the vacuum value at infinity. In principle, we could have $f(0) = N_f\pi$ for any non-zero integer N_f, but solutions with $N_f > 1$ have rather high energy and so we only consider $N_f = 1$.

Thus, the ansatz depends on a holomorphic map between two-spheres. Any holomorphic map of finite topological charge can be written as a rational map

$$R(z) = \frac{p(z)}{q(z)}, \tag{5}$$

where p and q are polynomials in z. The topological charge, N_R, of the map is equal to the algebraic degree and this, in turn, is given by the maximal degree of the two polynomials.

The easiest way to calculate the energy of an ansatz field is to use the geometric formulation of the Skyrme model [10]. A Skyrme field is a map between three-manifolds with metrics and so there is a strain tensor. This is given by

$$D_{ij} = -\frac{1}{2}\mathrm{Tr}\left(R_i R_j\right). \tag{6}$$

The static energy, E, and the baryon number, B, of a Skyrme field can be written in terms of the eigenvalues, λ_1^2, λ_2^2 and λ_3^2, of this tensor:

$$E = \int \left(\lambda_1^2 + \lambda_2^2 + \lambda_3^2 + \lambda_1^2\lambda_2^2 + \lambda_2^2\lambda_3^2 + \lambda_1^2\lambda_3^2\right), \tag{7}$$

$$B = \frac{1}{2\pi^2}\int \lambda_1\lambda_2\lambda_3. \tag{8}$$

The strain tensor of the ansatz field (3) can be calculated to give

$$B = \frac{2}{\pi}\int \left(-f'\sin^2 f\right)\mathrm{d}r \; \frac{1}{4\pi}\int \left(\frac{1+|z|^2}{1+|R|^2}\left|\frac{\mathrm{d}R}{\mathrm{d}z}\right|\right)^2 \frac{2i\;\mathrm{d}z\mathrm{d}\bar{z}}{(1+|z|^2)^2}, \tag{9}$$

$$= N_R, \tag{10}$$

where N_R is the degree of the rational map.

Similarly, the energy E is given by

$$E = 4\pi\int \left(f'^2 r^2 + 2N_R(f'^2+1)\sin^2 f + \mathcal{I}\;\frac{\sin^4 f}{r^2}\right)\mathrm{d}r, \tag{11}$$

where

$$\mathcal{I} = \frac{1}{4\pi}\int \left(\frac{1+|z|^2}{1+|R|^2}\left|\frac{\mathrm{d}R}{\mathrm{d}z}\right|\right)^4 \frac{2i\;\mathrm{d}z\mathrm{d}\bar{z}}{(1+|z|^2)^2}. \tag{12}$$

Thus, the minimum energy ansatz field is found by choosing polynomials p and q which minimize $\mathcal{I}$ and then calculating the shape function f numerically. These minimum energy ansatz fields have been calculated for all the known Skyrmions and are found to have energies that exceed the true, numerically determined, minima [7, 9] by less than three percent.

1.2 The Rational Map Ansatz and Negative Baryon Density

The accuracy of the ansatz is established by observing how close in energy the minimum energy ansatz configurations are to the true minima. In other words, it is not known whether the ansatz fields resemble the true fields in regions where the energy density is low. In fact, for the approximate fields calculated within the ansatz, the region of zero baryon density has a rather special structure. There are $2B-2$ radial half-lines which meet at the origin and extend out to infinity. The zeros of the baryon density correspond to the folds in the Skyrme fields, considered as maps between three-spheres. Line-like zeros are not generic. It is possible that these non-generic zeros are a natural consequence of minimizing the Skyrme energy [11, 12]. However, it may be that this is a weakness of the rational map ansatz and Skyrmions have a more generic folding structure.

If it is a weakness, it is not a very serious one. Most current interest is in finding minimum energy Skyrme configurations. However, the issue of determining the structure of Skyrme fields in the regions where there is little energy may be of some practical importance, for example, in calculations in which the Skyrmion fields are used as backgrounds for fermion excitations modeling heavy flavours, see [13].

In this paper, we consider the consequences of generalizing the rational map ansatz to include a larger class of maps. These maps permit a more natural, though not wholly generic, folding structure. This generalized ansatz is not as convenient as the original one. However, it does result in ansatz fields which are even closer to the true minima.

Our interest in this problem is partly motivated by BPS monopoles. There are many interesting similarities between Skyrmions and BPS monopoles. For example, there are two rational map descriptions of monopoles [14, 15], and it is widely believed that the space of attracting Skyrmions is related to the space of monopoles. It was discovered in [16] that the tetrahedral 3-monopole has a negative multiplicity Higgs zero. Subsequent examination revealed that the octahedral 5-monopole also has extra zeros but the cubic 4-monopole does not [17].

There is evidence that this pattern is mimicked by Skyrmions for $B = 3$ and 4. These Skyrmions were studied in [18] using the Atiyah-Manton ansatz [19]. It was observed that there is no negative baryon density in the approximate 4-Skyrmion, but there is in the approximate 3-Skyrmion case. In the approximate 3-Skyrmion there is a region of negative baryon density surrounding the origin. This extends out along four thin tubes which twice pinch to points and then widen at very large distance until they merge and form another region of negative baryon density at spatial infinity.

In this paper, we generalize the rational map ansatz so that there can be negative baryon density. We calculate ansatz fields that approximate the true minima more closely than the original rational map ansatz. The ansatz for the 3-Skyrmion has tubes of negative baryon density extending out from the origin; the ansatz for the 4-Skyrmion does not. Furthermore, there is an octahedrally symmetric $B = 5^*$ saddle-point configuration. The ansatz for this saddle point also has negative baryon density.

Thus, our investigation adds to the evidence that there may be regions of negative baryon density in certain Skyrmions. This occurs in those examples where the corresponding monopole has negative multiplicity Higgs zeros. Of course, our conclusions are based on an ansatz and the true solution does not necessarily possess the same singularity structure. Unfortunately, it is difficult to observe negative baryon density directly in the numerical solutions.

1.3 Singularities of Differentiable Maps

The theory of singularities deals with smooth maps between manifolds. One of its main aims is to classify the points where the Jacobian of a map does not have maximal rank. These are the singularities. Some singularities are unstable, in the sense that a small perturbation of the map can alter the nature of the singularity. For maps between low dimensional manifolds, there is only a small number of stable singularities. In this section, we describe the three stable singularities of smooth maps between three-dimensional manifolds. We will follow [20].

Let $f : M \to N$ be a map from a three-dimensional manifold M to a three-dimensional manifold N. Locally, there are coordinates $\{y_1, y_2, y_3\}$ on N and $\{x_1, x_2, x_3\}$ on M so that

$$\begin{aligned} y_1 &= f_1(x_1, x_2, x_3), \\ y_2 &= f_2(x_1, x_2, x_3), \\ y_3 &= f_3(x_1, x_2, x_3). \end{aligned} \tag{13}$$

The matrix $J = (\partial f_i/\partial x_j)$ is the Jacobian matrix of the map. The singularities are the points where $\det J = 0$. There are only three stable singularities: folds, cusps and swallowtails. These are described by giving their normal forms. The normal form is a standard choice of coordinates for the neighbourhood of the singularity. Any stable singularity can be expressed locally in terms of the corresponding normal form by a smooth change of variables.

The simplest singularity is the fold, which can be visualized as the line along which a piece of paper has been folded. A fold has the normal form:

$$\begin{aligned} y_1 &= x_1^2, \\ y_2 &= x_2, \\ y_3 &= x_3. \end{aligned} \tag{14}$$

It is worth considering the number of preimages of the map. For points of N with $y_1 > 0$ there are two preimages, whereas for points with $y_1 < 0$ there are no preimages. The fold is located at $y_1 = 0$, which has one preimage. Restricted to the set of points $y_1 = 0$, f maps the x_2x_3-plane onto the y_2y_3-plane.

The Jacobian matrix of this map is:

$$J = \begin{pmatrix} 2x_1 & 0 & 0 \\ 0 & 1 & 0 \\ 0 & 0 & 1 \end{pmatrix}. \tag{15}$$

It is singular at $x_1 = 0$, which, of course, is the location of the fold. The rank of the Jacobian matrix at the fold is two. In fact, this is true of all three stable singularities. Any singularity with a rank one or rank zero Jacobian matrix is unstable.

Two folds can end on a cusp. This has the normal form:

$$\begin{aligned} y_1 &= x_1^3 + x_1x_2, \\ y_2 &= x_2, \\ y_3 &= x_3. \end{aligned} \tag{16}$$

In order to get a better understanding of this singularity, we calculate the Jacobian matrix:

$$J = \begin{pmatrix} 3x_1^2 + x_2 & x_1 & 0 \\ 0 & 1 & 0 \\ 0 & 0 & 1 \end{pmatrix}. \tag{17}$$

J does not have maximal rank for $x_1^2 = -x_2/3$. This is a pair of folds. The cusp occurs at the line $(0, 0, x_3)$ where the two folding surfaces $(\pm\sqrt{-x_2/3}, x_2, x_3)$ meet.

The most complicated stable singularity is called the swallowtail and its normal form is

$$\begin{aligned} y_1 &= x_1^4 + x_1^2 x_2 + x_1 x_3, \\ y_2 &= x_2, \\ y_3 &= x_3. \end{aligned} \tag{18}$$

In this case, the Jacobian matrix is given by

$$J = \begin{pmatrix} 4x_1^3 + 2x_1 x_2 + x_3 & x_1^2 & x_1 \\ 0 & 1 & 0 \\ 0 & 0 & 1 \end{pmatrix}. \tag{19}$$

The points of the folds satisfy the equation $x_3 = -4x_1^3 - 2x_1 x_2$. The folds meet to form four cusp lines which meet at the origin. The origin is the swallowtail.

This classification is known as Whitney's Theorem. This theorem states that a map of a three-dimensional manifold to a three-dimensional manifold is stable at a point if, and only if, the map can be described in local coordinates in one of the four forms: a regular point with $y_1 = x_1$, $y_2 = x_2$ and $y_3 = x_3$ or one of the three singular forms given above. Furthermore, maps with stable singularities are dense in the space of all smooth maps: any map can be approximated arbitrarily closely by a map with stable singularities.

2 Folding and Rational Maps

We begin this section by showing that the simplest singularity of the rational map ansatz is unstable. This will lead us to introduce the non-holomorphic rational map ansatz in the following section. Furthermore, we show that for $B > 1$ there is an unstable singularity at the origin.

In the holomorphic rational map ansatz there is a map from $\mathbf{R}^3$ to S^3 which maps $(r, z, \bar{z})$ to $(f(r), R(z), \bar{R}(\bar{z}))$. Away from the origin, we can define local coordinates $\{\mathrm{Re}(z), \mathrm{Im}(z), x_3\}$ and $\{y_1, y_2, y_3\}$ such that

$$\begin{aligned} y_1 &= \mathrm{Re}(R), \\ y_2 &= \mathrm{Im}(R), \\ y_3 &= x_3. \end{aligned} \tag{20}$$

The simplest rational map with a singularity is

$$R(z) = z^2 \tag{21}$$

which gives

$$\begin{aligned} y_1 &= x_1^2 - x_2^2, \\ y_2 &= 2x_1 x_2, \\ y_3 &= x_3. \end{aligned} \tag{22}$$

The Jacobian matrix has rank one for the line $(0, 0, x_3)$. This is not one of the stable singularities.

Let us consider small perturbations around (21). Adding terms proportional to z only shifts the singularity. Therefore, we consider the following map:

$$R(z, \bar{z}) = z^2 + 2\epsilon\bar{z}. \tag{23}$$

Since multiplying ϵ by a phase $e^{i\phi}$ only rotates the singularities by ϕ, we can take ϵ to be real. Using real coordinates, the Jacobian matrix can be written as:

$$J = \begin{pmatrix} 2x_1 + 2\epsilon & -2x_2 & 0 \\ 2x_2 & 2x_1 - 2\epsilon & 0 \\ 0 & 0 & 1 \end{pmatrix}. \tag{24}$$

The Jacobian matrix is singular for $x_1^2 + x_2^2 = \epsilon^2$. Therefore, the singular points lie on a cylinder with radius ϵ. They can be parametrized by $x_1 = \epsilon\cos\alpha$ and $x_2 = \epsilon\sin\alpha$ for $\alpha \in [0, 2\pi]$, x_3 is arbitrary. Restricting the map to the singular surface, labeled by α and x_3, we can calculate the cusp lines. The surface is singular where

$$\frac{dy_1}{d\alpha} = \frac{dy_2}{d\alpha} = \frac{dy_3}{d\alpha} = 0, \tag{25}$$

therefore, the cusps form lines where α is zero, $2\pi/3$ or $4\pi/3$, and x_3 is arbitrary.

In Fig. 1, we show the image of a set of concentric circles of radius ρ in the x_1x_2-plane. By rescaling space and target space coordinates, the value of ϵ can be changed. For convenience, we set $\epsilon = 1$ in the figure. For small radius, ρ, the $\bar{z}$ term is dominant and the image of the circle is a deformed circle. As the radius increases, the circle becomes more and more deformed. The $\rho = 1$ circle maps to the singular curve. This curve has three spikes. The points of these spikes are the cusps and running between them are three folds. Above this value of ρ, the map folds back on itself. The points inside the fold have four preimages: a $\rho < 1$ preimage with negative Jacobian and three $\rho > 1$ preimages with positive Jacobians. Eventually, the image circle passes completely through the folding region: for $\rho > 3$ the image is a trefoil shape. Every point outside the fold has just two preimages, each with positive Jacobian.

In general, the map $R(z) = z^n$ for $n \geq 2$ has an unstable singularity on the x_3-axis. This unstable singularity can be removed by adding an anti-holomorphic perturbation. The perturbed map $R(z) = z^n + n\epsilon\bar{z}$ has a folding surface at $z = \epsilon\exp(i\alpha)$. There are $n+1$ cusps which are located at $\alpha = 2\pi k/(n+1)$ where $k = 0, \ldots, n$. This map possesses a natural C_{n+1}-symmetry, which maps the cusps into each other.

It is worth noting that z^2 is a stable singularity within the set of holomorphic functions, whereas z^n for $n > 2$ is unstable even as a holomorphic map. Therefore, we do not expect the latter singularities to occur for a generic holomorphic map.

Let us also consider the singularities of the rational map ansatz at the origin. Locally, the shape function can be written as

$$f(r) = \pi - Ar^\nu + O(r^{\nu+1}), \tag{26}$$

where A is an arbitrary positive constant and

$$\nu = -\frac{1}{2} + \frac{1}{2}\sqrt{8B+1}. \tag{27}$$

For $B = 1$ this exponent is equal to one. This means that the Jacobian has full rank at the origin. However, for $B > 1$ the exponent ν is greater than one. In this case the Jacobian of

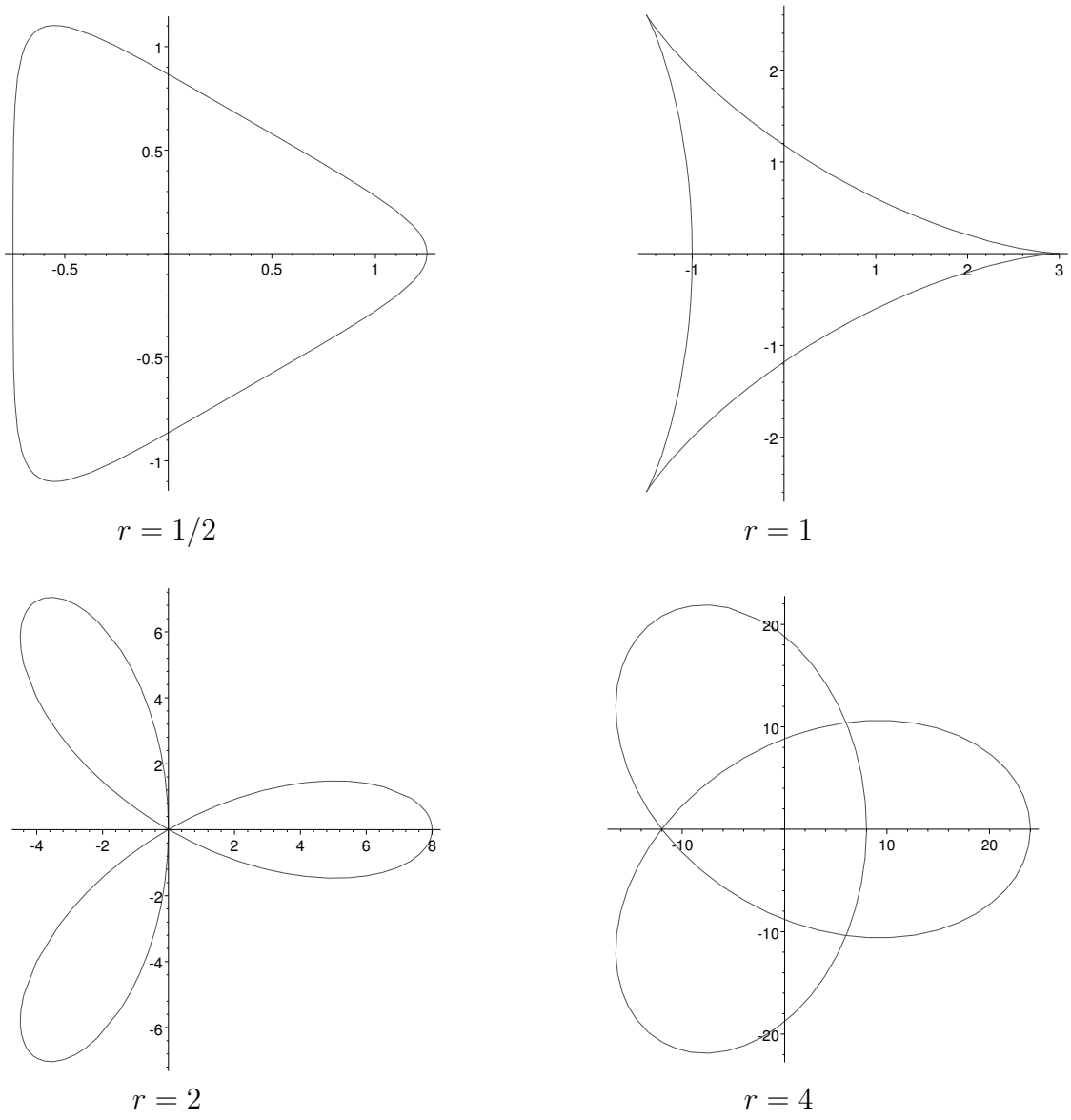

Figure 1: The image of concentric circles $z = \rho e^{i\phi}$ of various radii ρ under $R(z, \bar{z}) = z^2 + 2\bar{z}$. Note that the scale is different for each graph.

the rational map ansatz has rank zero. Moreover, the derivative $R_z(z)$ vanishes for certain values of z. Therefore, lines of degenerate singularities with rank one Jacobian matrices meet at the origin. Here they form an even more degenerate singularity with a rank zero Jacobian matrix. In Sect. 3.2, we argue that for $B = 3$ there is a more likely singularity configuration close to the origin.

2.1 Non-Holomorphic Rational Maps

The rational map ansatz restricts the ansatz fields in three different ways. It requires that concentric two-spheres around the origin in space are mapped to two-spheres in SU_2. It also requires that this map is the same for all concentric two-spheres, and it requires that the

map between two-spheres is a holomorphic map. Our intention here is to relax the third of these conditions. We will consider a larger class of maps. The maps we will consider will be rational maps in the sense that they will have the form of a ratio between polynomials. However, the polynomials will depend on $\bar{z}$ as well as z, so they will not be holomorphic maps.

To begin with, we consider the ansatz

$$U(r, z, \bar{z}) = \exp\left(if(r)\ \widehat{\mathbf{n}}_R \cdot \boldsymbol{\sigma}\right), \tag{28}$$

where, as before,

$$\widehat{\mathbf{n}}_R = \frac{1}{1+|R|^2}(2\mathrm{Re}(R), 2\mathrm{Im}(R), 1-|R|^2) \tag{29}$$

but, without assuming R is holomorphic,

$$R = R(z, \bar{z}). \tag{30}$$

In order to derive the energy, E, we calculate the eigenvalues λ_1^2, λ_2^2 and λ_3^2 of the strain tensor (6). The strain tensor can be written as

$$(D_{ij}) = \begin{pmatrix} f'^2 & 0 & 0 \\ 0 & A\left(R_z + R_{\bar{z}}\right)\left(\bar{R}_z + \bar{R}_{\bar{z}}\right) & iA\left(R_z\bar{R}_z - R_{\bar{z}}\bar{R}_{\bar{z}}\right) \\ 0 & iA\left(R_z\bar{R}_z - R_{\bar{z}}\bar{R}_{\bar{z}}\right) & -A\left(R_z - R_{\bar{z}}\right)\left(\bar{R}_z - \bar{R}_{\bar{z}}\right) \end{pmatrix}, \tag{31}$$

where

$$A = \left(\frac{1+|z|^2}{1+|R|^2}\frac{\sin f}{r}\right)^2, \tag{32}$$

and has eigenvalues

$$\begin{aligned} \lambda_1^2 &= f'^2, \\ \lambda_2^2 &= \left(\frac{|R_z| + |R_{\bar{z}}|}{r}\frac{1+|z|^2}{1+|R|^2}\sin f\right)^2, \\ \lambda_3^2 &= \left(\frac{|R_z| - |R_{\bar{z}}|}{r}\frac{1+|z|^2}{1+|R|^2}\sin f\right)^2. \end{aligned} \tag{33}$$

Notice that λ_2^2 and λ_3^2 are only equal if $R_{\bar{z}} = 0$, or $R_z = 0$. In the first case, the energy of the holomorphic rational map ansatz (11) is reproduced. The second case corresponds to a purely anti-holomorphic ansatz and is just the holomorphic ansatz composed with a reflection.

Using equation (7) the energy E can be rewritten as

$$E = 4\pi \int \left(r^2 f'^2 + 2\mathcal{J}(f'^2+1)\sin^2 f + \mathcal{I}\frac{\sin^4 f}{r^2}\right) \mathrm{d}r, \tag{34}$$

where $\mathcal{I}$ and $\mathcal{J}$ are given by:

$$\mathcal{J} = \frac{1}{4\pi}\int \left(\frac{(|R_z|^2 + |R_{\bar{z}}|^2)(1+|z|^2)^2}{(1+|R|^2)^2}\right)\frac{2i\ \mathrm{d}z\mathrm{d}\bar{z}}{(1+|z|^2)^2} \tag{35}$$

and

$$\mathcal{I} = \frac{1}{4\pi}\int \left(\frac{(|R_z|^2 - |R_{\bar{z}}|^2)(1+|z|^2)^2}{(1+|R|^2)^2}\right)^2\frac{2i\ \mathrm{d}z\mathrm{d}\bar{z}}{(1+|z|^2)^2}. \tag{36}$$

As in the holomorphic ansatz, $\mathcal{I}$ is essentially the integral of the square of the Jacobian. However, $\mathcal{J}$ is not the integral of the Jacobian of R.

There is a close relationship between this energy functional and the baby Skyrme model on a two-sphere. The baby Skyrme model [21, 22] is a sigma-model in (2+1) dimensions with a fourth order Skyrme-like interaction. The baby-Skyrme model on the two-sphere is of independent interest, primarily because there is a phase transition as the radius of the sphere is changed [23, 24].

On a unit two-sphere, the baby Skyrme fields map S^2 to S^2 and the energy functional is of the form $g_1\mathcal{J} + g_2\mathcal{I}$ where g_1 and g_2 are coupling constants. $\mathcal{J}$ is the sigma-model energy and $\mathcal{I}$ is the Skyrme energy. For a given shape function, f, the energy E in (34) is of this form with g_1 and g_2 calculated by integrating the shape function over r.

Obviously, it would be possible to regard the holomorphic maps between two-spheres as ansätze for baby-Skyrme fields. For a holomorphic map, $\mathcal{J}$ is equal to the topological degree. Thus, the holomorphic map which minimizes $\mathcal{I}$ gives the best approximation to the energy minimizing baby-Skyrme field. In other words, to find the baby-Skyrme energy minimizing holomorphic map, the values of g_1 and g_2 need not be known. This is one of the reasons why the original rational map ansatz is so convenient to use: the rational map is found first and the shape function is then determined numerically.

For more general maps we need to employ an iterative algorithm. Firstly, using the $\mathcal{I}$ minimizing holomorphic rational map, a shape function can be calculated numerically. This gives provisional values for the coupling constants g_1 and g_2. The next step is to minimize the baby-Skyrme energy with these values of g_1 and g_2. This determines a new map between the Riemann spheres. The original shape function is not optimized for this new map, so a new shape function must be calculated. A new profile function gives new coupling constants and so the whole procedure has to be iterated. In practice, this procedure is simplified by the fact that we only consider one-parameter families of non-holomorphic rational maps.

Another major advantage of using holomorphic maps is that there is only a finite-dimensional family of holomorphic maps of given topological degree. In contrast, the space of general maps between two-spheres of a given degree is infinite dimensional. One way to avoid this problem would be to minimize the baby-Skyrme model numerically. However, our interest here is in the folding behavior of minimum energy Skyrmions and so we would prefer to find an approximate analytic solution whose folding behavior we can analyze. For this reason, we will restrict our attention to maps of the form

$$R(z, \bar{z}) = \frac{p(z, \bar{z})}{q(z, \bar{z})}, \tag{37}$$

where p and q are polynomials in both z and $\bar{z}$. We will call the polynomial degree of this map (N_1, N_2), where N_1 is the maximal holomorphic degree of the polynomials p and q and N_2 is their maximal anti-holomorphic degree. By counting the number of preimages of a given value of R and taking into account the sign of the Jacobian at each preimage, it follows that a general map of this form has topological degree $N_1 - N_2$. Some maps will have a different degree because p and q may have a common factor. Maps of this type are called spurious.

According to formula (8), the baryon number is

$$B = \frac{2}{\pi}\int f' \sin^2 f \ \mathrm{d}r \ \frac{1}{4\pi}\int \frac{(|R_z|^2 - |R_{\bar{z}}|^2)(1+|z|^2)^2}{(1+|R|^2)^2}\frac{2i \ \mathrm{d}z\mathrm{d}\bar{z}}{(1+|z|^2)^2}. \tag{38}$$

B is no longer an integral over squares, as it was for the holomorphic rational map ansatz. It is possible that the baryon density could be locally negative. We will find that this is what happens for certain values of B.

2.2 Symmetric Non-Holomorphic Rational Maps

The Skyrmions that we are interested in are symmetrical: the 3-Skyrmion is tetrahedrally symmetric and the $B = 4$ is octahedrally symmetric [5]. Rather than minimizing the ansatz energy over the whole space of maps, we restrict our attention to maps that have the same symmetry as the numerically determined minimum energy solution.

An SO_3 rotation g acts on the Riemann sphere z as a Möbius transformation

$$z \mapsto g(z) = \frac{\alpha z + \beta}{-\bar{\beta} z + \bar{\alpha}}, \tag{39}$$

where $|\alpha|^2 + |\beta|^2 = 1$. There is also a Möbius action on the rational maps. A Möbius transformation of the rational map is equivalent to a global group transformation of the corresponding Skyrme fields. A Skyrme field is symmetric under a rotation, g, if the rotated fields are a global group transformation of the original fields. In the same way, the rational map $R(z, \bar{z})$ is symmetric under g if

$$R\left(g(z), \overline{g(z)}\right) = \frac{\alpha' R(z, \bar{z}) + \beta'}{-\overline{\beta}' R(z, \bar{z}) + \overline{\alpha}'}, \tag{40}$$

where α' and β' are not necessarily the same as α and β.

Symmetric non-holomorphic rational maps can be calculated using elementary representation theory. In this subsection, we describe this construction. In the next section, we will derive non-holomorphic rational maps for various B.

The Riemann sphere is isomorphic to $\mathbf{CP}^1$, the one-dimensional complex projective space. $\mathbf{CP}^1$ can be labeled by a pair of complex numbers $[u, v]$, where the square bracket indicates the relation

$$[u, v] \cong [\lambda u, \lambda v] \tag{41}$$

with $\lambda \in \mathbf{C}^\times$. These homogeneous coordinates, u and v, are related to the inhomogeneous coordinate by $z = u/v$. The rotation group acts linearly on the homogenous coordinates and, so, it is easier to use these coordinates to describe the representation theory. However, we switch to inhomogeneous coordinates whenever they are more convenient. Similarly, we can label the Riemann sphere by the complex conjugates of u and v, $[\bar{u}, \bar{v}]$, also subject to relation (41). A non-holomorphic rational map takes the form

$$R(u, v, \bar{u}, \bar{v}) = \left[p\left(u, v, \bar{u}, \bar{v}\right), q\left(u, v, \bar{u}, \bar{v}\right)\right]. \tag{42}$$

This rational map must be well-defined under the relation (41).Therefore, p and q have to be homogeneous: they are of the form

$$p\left(u, v, \bar{u}, \bar{v}\right) = \sum_{i=0}^{N_1} \sum_{j=0}^{N_2} a_{ij} u^i v^{N_1 - i} \bar{u}^j \bar{v}^{N_2 - j}, \tag{43}$$

$$q\left(u, v, \bar{u}, \bar{v}\right) = \sum_{i=0}^{N_1} \sum_{j=0}^{N_2} b_{ij} u^i v^{N_1 - i} \bar{u}^j \bar{v}^{N_2 - j}. \tag{44}$$

It should be noted that the topological degree does not depend on the value of $N_1 + N_2$, it only depends on their difference. Choosing N_1 and N_2 corresponds to a truncation of the possible maps between Riemann spheres. This truncation is similar to truncating a Fourier expansion. In this paper we will consider non-holomorphic maps with N_2 equal one or two.

Under an SO_3 rotation about the unit vector $\widehat{\mathbf{n}}$ by an angle θ, the $[u, v]$ coordinates transform by an SU_2 transformation $\exp(i(\theta/2)\widehat{\mathbf{n}} \cdot \boldsymbol{\sigma})$. The SO_3 action on the Riemann sphere $[u, v]$ can now be written as:

$$\begin{aligned} u &\mapsto u' = (a_0 + ia_3)u + (a_2 + ia_1)v, \\ v &\mapsto v' = (-a_2 + ia_1)u + (a_0 - ia_3)v, \end{aligned} \tag{45}$$

where $a_i = n_i \sin(\theta/2)$ and $a_0 = \cos(\theta/2)$. The coordinates $[\bar{u}, \bar{v}]$ transform as the complex conjugate of (45). Let G be the double group of a finite subgroup of SO_3. The rational map $[p, q]$ is G invariant if an SU_2 transformation of $[u, v]$ and $[\bar{u}, \bar{v}]$ is equivalent to an SU_2 transformation of $[p, q]$.

A homogeneous polynomial of degree N in z transforms as $\mathbf{N + 1}$, the $(N+1)$-dimensional irreducible representation of SU_2. It follows that the homogeneous polynomial p of degree N_1 in z and degree N_2 in $\bar{z}$ transforms as $(\mathbf{N_1 + 1}) \otimes (\mathbf{N_2 + 1})$. This representation can be decomposed into irreducible representations of some finite group G. These decompositions can be calculated using the characters. Tables of these decompositions can be found, for example, in [25].

By decomposing the $(\mathbf{N_1 + 1}) \otimes (\mathbf{N_2 + 1})$ as a representation of G we can determine whether or not there is a G invariant degree (N_1, N_2) rational map. In fact, the rational map $[p, q]$ can be G-invariant in two different ways. One possibility is that

$$(\mathbf{N_1 + 1}) \otimes (\mathbf{N_2 + 1})|_G = E \oplus \text{ other irreducible representations of } G, \tag{46}$$

and $\{p, q\}$ form a basis for the two-dimensional irreducible representation E. This means p and q are transformed into linear combinations of each other under Möbius transformations of z. Moreover, by a choice of basis, these combinations are unitary. This is always possible, because every representation of a finite group is equivalent to a unitary representation, [26]. The second possibility is that

$$(\mathbf{N_1 + 1}) \otimes (\mathbf{N_2 + 1})|_G = A_1 \oplus A_2 \oplus \text{ other irreducible representations of } G, \tag{47}$$

and p is a basis for A_1, and q is a basis of A_2. Here, A_1 and A_2 are two different one-dimensional representations of G. In this case, there is a one-parameter family of G-symmetric rational maps: namely $R = [p, aq]$. The parameter a can be chosen to be real, because a Möbius transformation of R can change the phase of a.

Of course, there is also a one-parameter family when

$$(\mathbf{N_1 + 1}) \otimes (\mathbf{N_2 + 1})|_G = 2E \oplus \text{ other irreducible representations of } G \tag{48}$$

because, in this case, there is a one-parameter family of choices of an E inside $2E$. In order to construct a basis of this one-parameter family, we can construct a projector $P_{\alpha\beta}$. Given a representation ρ and a two-dimensional unitary representation $\rho^{(2)}_{\alpha\beta}$, the projector is given by

$$P_{\alpha\beta} = \frac{2}{|G|} \sum_{g \in G} \rho^{(2)}_{\alpha\beta}(g^{-1}) \rho(g). \tag{49}$$

For details of this construction, see [9, 27]. It is not always necessary to construct projectors. In the $B = 2$ case discussed below, the invariant map is calculated by direct calculation and in the $B = 3$ case it is derived from other, previously known, examples.

3 Skyrmions from Non-Holomorphic Rational Maps

In this section, we use non-holomorphic rational maps to approximate the Skyrmions with baryon number two to four. In each of these cases, there is a one-parameter family of maps with the correct symmetry. Once the approximating map is found, we can discuss the folding structure. We also consider the $B = 5^*$ octahedral saddle point which also has a one-parameter family of symmetric maps. It is more tractable than the 5-Skyrmion, because the 5-Skyrmion is not very symmetrical.

3.1 $B = 2$: the Torus

For $B = 2$, the holomorphic rational map which minimizes $\mathcal{I}$ is:

$$R(z) = z^2. \tag{50}$$

It has the same D_∞ symmetry as the true solution. There is an axial symmetry

$$R(e^{i\chi}z) = e^{2i\chi}R(z) \tag{51}$$

and a symmetry under rotation by π around an orthogonal axis

$$R\left(\frac{1}{z}\right) = \frac{1}{R\,(z)}. \tag{52}$$

The group theory methods discussed in the last section are not really needed here. The most general D_∞-symmetric map can be calculated by writing out the general $(3, 1)$ rational map and applying the symmetries (51) and (52). It is

$$R(z, \bar{z}) = \frac{az^2(z\bar{z} + 1) + bz^2(z\bar{z} - 1)}{a(z\bar{z} + 1) + b(-z\bar{z} + 1)}. \tag{53}$$

The true solution also has a reflection symmetry. In the holomorphic case, that reflection symmetry is $R(\bar{z}) = \overline{R(z)}$. If we impose the same symmetry for the non-holomorphic map, then the parameters a and b have to be real, up to a common phase. Moreover, since the pair (a, b) and $(\lambda a, \lambda b)$ gives rise to the same rational map for all $\lambda \in \mathbf{C}^\times$, we can set $a = \cos\theta$ and $b = \sin\theta$. The polynomials have been chosen such that the value $\theta = 0$ corresponds to the holomorphic rational $(2, 0)$ map. θ is in the range $[-\pi/2, \pi/2]$, because under $\theta \mapsto \theta + \pi$ both $\sin\theta$ and $\cos\theta$ change sign.

In Fig. 2, we show the value of $\mathcal{J}$ and $\mathcal{I}$ as a function of θ. There are two poles, one at $\theta = -\pi/4$ and another at $\theta = \pm\pi/2$. Both of these poles correspond to points where the maps are spurious. At $\theta = -\pi/4$, the cancellation of the common factor changes the topological degree:

$$R(z, \bar{z})|_{\theta=-\pi/4} = \frac{z}{\bar{z}}, \tag{54}$$

whereas, at $\theta = \pm\pi/2$ it does not:

$$R(z, \bar{z})|_{\theta=\pm\pi/2} = -z^2. \tag{55}$$

Thus, while the integrals are non-singular at $\theta = \pm\pi/2$, they diverge as this value of θ is approached. These poles are considered in detail in [27]. In [27], it is also shown that there is some negative baryon density only if $-\pi/2 < \theta < -\pi/4$ or $\pi/4 < \theta < \pi/2$.

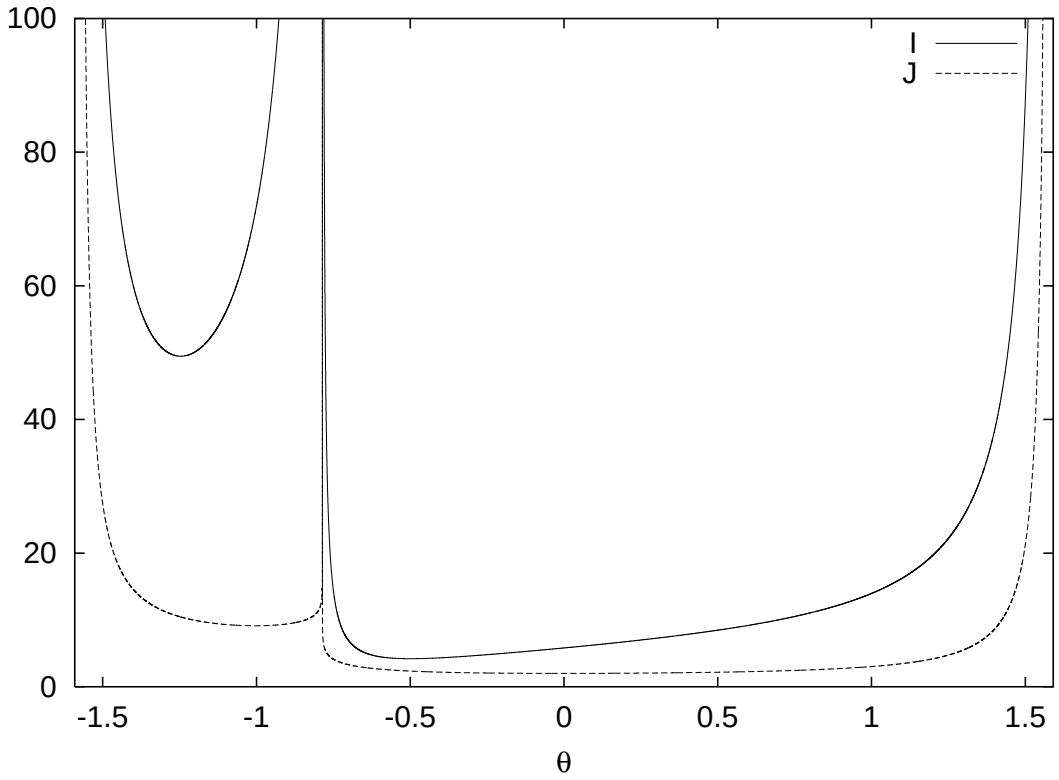

Figure 2: $\mathcal{I}$ and $\mathcal{J}$ as a function of θ for $B = 2$.

To find the best approximation to the true minimum, we calculate the value of θ which minimizes the energy. The energy is a combination of $\mathcal{I}$ and $\mathcal{J}$. The optimal value for $\mathcal{J}$ is at the holomorphic rational map value $\theta = 0$. However, $\mathcal{I}$ is minimal for $\theta \approx -0.503$. Minimizing energy (34) with respect to θ numerically, using the golden rule algorithm [28], gives an optimal value of $\theta \approx -0.202$. The energy per Skyrmion calculated with this method is $E/B \approx 1.191$. In contrast, for the holomorphic rational map $\theta = 0$, we obtain $E/B \approx 1.208$. The true value of the energy per Skyrmion is $E/B \approx 1.1791$. For the energy minimizing value of θ, the baryon density is positive everywhere except at the origin. Thus, we find that there is no negative baryon density for $B = 2$, even though there is a significant improvement in the energy. It seems that the axial symmetry stabilizes the unstable singularity.

3.2 $B = 3$: the Tetrahedron

The 3-Skyrmion has tetrahedral symmetry T. The holomorphic rational map ansatz is

$$\begin{aligned} p_T(z) &= -i\sqrt{3}z^2 + 1, \\ q_T(z) &= z^3 - i\sqrt{3}z, \end{aligned} \tag{56}$$

and $\{p_T, q_T\}$ is a basis for the E_2' in

$$\mathbf{4}|_T = E_2' \oplus E_3'. \tag{57}$$

The decompositions can be easily derived from the characters. Tables of these decompositions can also be found in, for example, [25]. For convenience, a short table is given in Table 1.

$$
\begin{aligned}
\mathbf{1}|_T &= A_1 \\
\mathbf{2}|_T &= E_1' \\
\mathbf{3}|_T &= F \\
\mathbf{4}|_T &= E_2' \oplus E_3' \\
\mathbf{5}|_T &= A_2 \oplus A_3 \oplus F \\
\mathbf{6}|_T &= E_1' \oplus E_2' \oplus E_3' \\
\mathbf{7}|_T &= A_1 \oplus 2F
\end{aligned}
$$

Table 1: The decomposition of irreducible representations of SU_2 as representations of T.

A_1	A_2	A_3	F	E_1'	E_2'	E_3'	$\otimes$
A_1	A_2	A_3	F	E_1'	E_2'	E_3'	A_1
	A_3	A_1	F	E_2'	E_3'	E_1'	A_2
		A_2	F	E_3'	E_1'	E_2'	A_3
			$A_1 \oplus A_2 \oplus A_3 \oplus 2F$	$E_1' \oplus E_2' \oplus E_3'$	$E_1' \oplus E_2' \oplus E_3'$	$E_1' \oplus E_2' \oplus E_3'$	F
				$A_1 \oplus F$	$A_2 \oplus F$	$A_3 \oplus F$	E_1'
					$A_3 \oplus F$	$A_1 \oplus F$	E_2'
						$A_2 \oplus F$	E_3'

Table 2: A multiplication table for the irreducible representations of T.

Here, we are interested in the non-holomorphic maps of degree $(4, 1)$. These correspond to the 10-dimensional representation $\mathbf{5} \otimes \mathbf{2}$ and can be decomposed into

$$
\begin{aligned}
\mathbf{5} \otimes \mathbf{2} &= \mathbf{6} \oplus \mathbf{4}, \\
(\mathbf{6} \oplus \mathbf{4})|_T &= {E_1}' \oplus 2{E_2}' \oplus 2{E_3}'.
\end{aligned} \tag{58}
$$

Both $\{1, z\}$ and $\{1, \bar{z}\}$ are a basis of the irreducible representation ${E_1}'$ of T. When they are multiplied, they decompose into $A_1 \oplus F$. For convenience, a multiplication table for the tetrahedral group is given in Table 2.

A basis for this A_1 is:

$$
k = z\bar{z} + 1. \tag{59}
$$

Furthermore, because $A_1 \otimes E_2' = E_2'$, $\{kp_T, kq_T\}$ is a basis for an E_2' inside $\mathbf{5} \otimes \mathbf{2}$. Explicitly, this basis is

$$
\begin{aligned}
p_1(z, \bar{z}) &= i\sqrt{3}z^3\bar{z} + i\sqrt{3}z^2 - z\bar{z} - 1, \\
q_1(z, \bar{z}) &= z^4\bar{z} + z^3 - i\sqrt{3}z^2\bar{z} - i\sqrt{3}z.
\end{aligned} \tag{60}
$$

The rational map for this basis is spurious: $[p_1, q_1] = [kp_T, kq_T] = [p_T, q_T]$. The common factor of k cancels. However, when we have a second independent basis, $\{p_2, q_2\}$, we will be able to form non-spurious linear combinations involving p_1 and q_1.

To find an independent pair of basis vectors in $2E_2'$, we use the A_2 in $\mathbf{5}|_T = A_2 + A_3 + F$. A basis for this A_2 is the Klein polynomial

$$
k_f = z^4 - 2i\sqrt{3}z^2 + 1. \tag{61}
$$

This is often called the face polynomial, because its zeros are the face points of a tetrahedron. Of course, the distinction between this and the vertex polynomial is a matter of convention. Now, $A_2 \otimes E_1' = E_2'$ and so the required basis for E_2' can be found by multiplying k_f by $[1, -\bar{z}]$. Thus, a second basis is given by

$$\begin{aligned} p_2(z,\bar{z}) &= z^4 - 2i\sqrt{3}z^2 + 1 \\ q_2(z,\bar{z}) &= -z^4\bar{z} + 2i\sqrt{3}z^2\bar{z} - \bar{z}. \end{aligned} \tag{62}$$

As with the other basis pair, the rational map for this basis is spurious: $[p_2, q_2] = [k_f, k_f\bar{z}] = [1, -\bar{z}]$.

A general T-symmetric non-holomorphic rational map of degree 3 is given by

$$R(z,\bar{z}) = \frac{\cos\theta p_1 + \sin\theta\ \mathrm{e}^{i\phi}p_2}{\cos\theta q_1 + \sin\theta\ \mathrm{e}^{i\phi}q_2}. \tag{63}$$

The two angles θ and ϕ parameterize all maps. When $\theta = 0$ this map is spurious and reduces to the tetrahedrally symmetric degree $(3,0)$ rational map studied in [9]. $\theta = \pm\pi/2$ is also spurious, here the map reduces to a degree $(0,1)$ map. In this case, the cancellation changes the topological degree of the map. It is expected that $\mathcal{I}$ tends to infinity as this value of θ is approached.

For $\phi = 0$, the map also has an additional reflection symmetry and the symmetry group becomes T_d. Since the numerically determined minimum seems to have this symmetry, it is expected that the best result from the rational map ansatz will come from $\phi = 0$. We have confirmed this and will restrict our discussion to this case.

In Fig. 3, we display $\mathcal{I}$ and $\mathcal{J}$ as a function of the angle θ. The minimum of $\mathcal{J}$ is still at the rational map value $\theta = 0$ with $\mathcal{J} = 3$. However, the minimum of $\mathcal{I}$ is at $\theta \approx 0.252$ with $\mathcal{I} \approx 11.04$. The minimum of the energy can now be calculated by varying θ, using a simple minimization scheme in which the shape function is recalculate at each step. We obtain $E/B \approx 1.160$ for $\theta \approx 0.155$. The holomorphic rational map value is $E/B \approx 1.184$, whereas the exact solution has $E/B \approx 1.1462$. Therefore, the non-holomorphic rational map ansatz is a significant improvement.

Furthermore, there are regions of negative baryon density. In the holomorphic ansatz the singularities of the rational maps correspond to points on the face centres of a tetrahedron. Let us consider the baryon density near these points. The determinant of the Jacobian of the map R is proportional to the baryon density in (38):

$$B_R = \frac{(|R_z|^2 - |R_{\bar{z}}|^2)(1+|z|^2)^2}{4\pi(1+|R|^2)^2}, \tag{64}$$

where we have integrated over r using the boundary conditions on f.

It is convenient to reorient the map (63) using the Möbius transformation

$$z \mapsto \frac{2z + (\sqrt{3}-1)(1+i)}{(1-\sqrt{3})(1-i)z + 2}. \tag{65}$$

If the holomorphic map (56) is rotated in this way, it is singular at $z = 0$, that is, B_R for the holomorphic map vanishes at $z = 0$. If we rotate the non-holomorphic map (63) by the same Möbius transformation and expand B_R in terms of z and $\bar{z}$ we obtain

$$B_R \approx -0.17 + 10.8z\bar{z}, \tag{66}$$

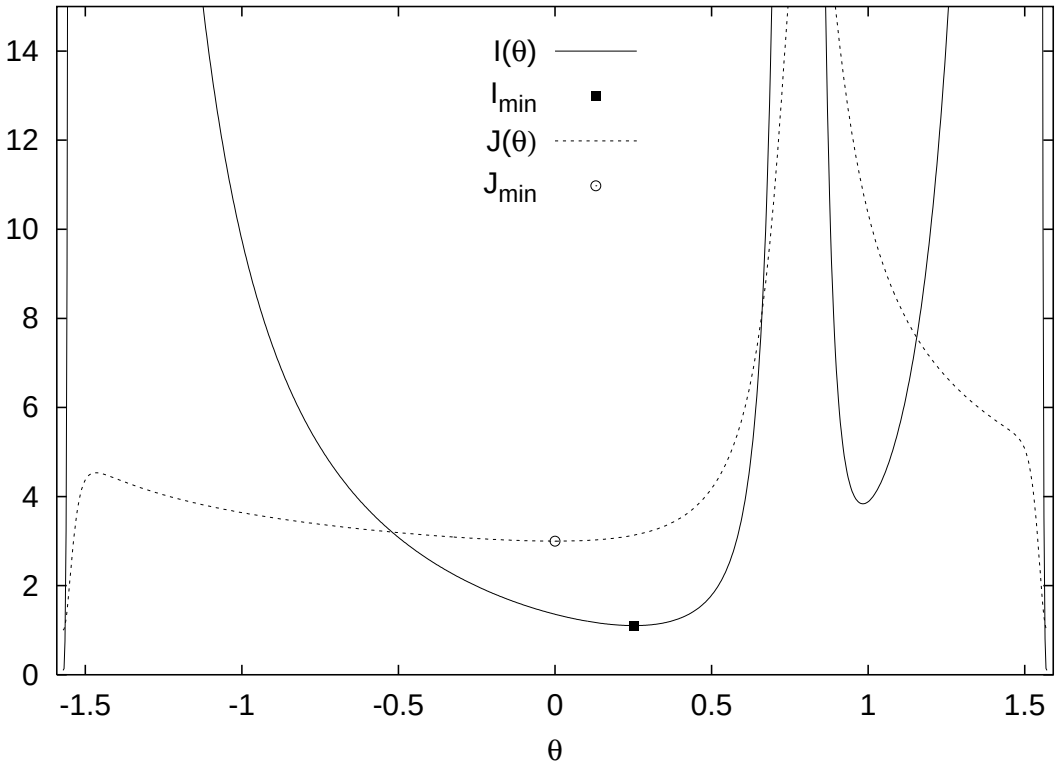

Figure 3: $\mathcal{I}$ and $\mathcal{J}$ as a function of θ for $B = 3$. Here $\mathcal{I}$ is rescaled by a factor of 10.

where θ has been set to the energy minimizing value 0.155. For $z = 0$ the baryon density is negative and to lowest order in z and $\bar{z}$ the folds lie on a circle around the origin in the z-plane. Thus, the non-holomorphic rational map ansatz predicts tubes of negative baryon density. In fact, the total negative baryon density, B_-, can be calculated numerically. It is $B_- \approx 0.000089$.

Finally, we discuss the general singularity structure of the 3-Skyrmion. All the singularities are of z^2 type and break up into three cusps connected by folds. This is compatible with the tetrahedral symmetry. Therefore, a 3-Skyrmion consists of four tubes of folds, one through each of the faces of the tetrahedron. Each of these tubes contains three cusp lines. There are 12 cusp lines in total.

Unfortunately, it is difficult to directly examine the Skyrmion at the origin and at infinity using these methods. It is possible to speculate on what the singularity structure is, based on the assumption that the singularities are all generic.

From the discussion in Sect. 1.3 we know that four cusp lines meet in a swallowtail. The cusp lines have to respect the tetrahedral symmetry. If the singularities are generic, they must meet in a swallowtail. Therefore, the 12 cusp lines cannot meet at the origin but have to split up earlier.

Considering only the cusp structure, one possible configuration, would be that the three cusp lines of each fold tube meet in a swallowtail, resulting in one further cusp. The simplest tetrahedrally symmetric configuration would be that this cusp meets similar cusps of the remaining three fold tubes at the origin. However, we also know that the instanton approximation to the 3-Skyrmion has negative baryon density at the origin [18], whereas

this possible configuration does not, because it has a singularity at the origin.

The following configuration is more likely. Each cusp of the fold splits up into three cusps at a swallowtail at some distance from the origin. Two of the cusp lines connect to the remaining two swallowtails of the fold tube. The last cusp line connects to the nearest swallowtail belonging to a different fold tube. This configuration is again tetrahedrally symmetric. Moreover, at the origin the baryon density is non-zero. We will call the cusp lines which follow the fold tubes *long cusp lines*, the cusp lines which connect swallowtails of the same fold tube *short cusp lines* and the cusp lines which connect swallowtails of different fold tubes *medium cusp lines*. In this configuration there are 12 long cusp lines, six medium cusp lines, and 12 short cusp lines. Note that the medium cusp lines lie on the edges of a tetrahedron.

In order to decide the sign of the baryon density at the origin, it is worth considering the folds of this configuration. Folds separate positive from negative baryon density. Moreover, precisely two folds end in one cusp. There are three folding surfaces in each fold tube. Each of these folding surfaces ends in two long cusp lines and one short cusp line. There are four additional folding surfaces, which can be visualized as the sides of a tetrahedron. Each of these folding surfaces ends in three medium cusp lines and three short cusp lines. These are all the folding surfaces because precisely two folding surfaces end in each of the cusps. Therefore, the baryon density at the origin has the same sign as the baryon density inside the fold tubes.

Thus, the baryon density at the origin is negative, as it is in the instanton ansatz, [18]. In the instanton configuration the negative baryon density tubes pinch at two points. It is not possible to decide using our methods whether this is a peculiarity of the instanton ansatz or a feature of the 3-Skyrmion.

3.3 $B = 4$: the Cube

The minimum energy $B = 4$ configuration looks like a cube and has octahedral symmetry O. The corresponding invariant holomorphic map is

$$\begin{aligned} p_O(z) &= 2\sqrt{3}z^2, \\ q_O(z) &= z^4 + 1. \end{aligned} \tag{67}$$

These polynomials are a basis of the E in

$$\mathbf{5}|_O = E \oplus F_2. \tag{68}$$

As before, these decompositions can be easily calculated, but, for convenience, a table of them is given in Table 3.

In the tetrahedral case, there was a unique invariant $(3, 0)$ map and a one-parameter family of $(4, 1)$ maps. The same thing does not happen here: if we consider $(5, 1)$ maps we obtain

$$\begin{aligned} \mathbf{6} \otimes \mathbf{2} &= \mathbf{7} \oplus \mathbf{5}, \\ (\mathbf{7} \oplus \mathbf{5})|_O &= A_2 \oplus E \oplus F_1 \oplus 2F_2, \end{aligned} \tag{69}$$

and the E is just the spurious map $[kp_O, kq_O] = [p_O, q_O]$. $k = 1 + z\bar{z}$ is the invariant polynomial discussed earlier. In other words, the only invariant $(5, 1)$ map reduces to the holomorphic map.

$$
\begin{aligned}
\mathbf{1}|_O &= A_1 \\
\mathbf{2}|_O &= E_1' \\
\mathbf{3}|_O &= F_1 \\
\mathbf{4}|_O &= G' \\
\mathbf{5}|_O &= E \oplus F_2 \\
\mathbf{6}|_O &= E_2' \oplus G' \\
\mathbf{7}|_O &= A_2 \oplus F_1 \oplus F_2 \\
\mathbf{8}|_O &= E_1' \oplus E_2' \oplus G' \\
\mathbf{9}|_O &= A_1 \oplus E \oplus F_1 \oplus F_2
\end{aligned}
$$

Table 3: The decomposition of the irreducible representations of SU_2 as representations of O.

This means that, in order to derive a one-parameter family of invariant rational maps, we need to consider degree $(6,2)$:

$$
\begin{aligned}
\mathbf{7} \otimes \mathbf{3} &= \mathbf{9} \oplus \mathbf{7} \oplus \mathbf{5}, \\
(\mathbf{9} \oplus \mathbf{7} \oplus \mathbf{5})|_O &= A_1 \oplus A_2 \oplus 2E \oplus 2F_1 \oplus 3F_2.
\end{aligned} \tag{70}
$$

Thus, there is a one-parameter family corresponding to the $2E$.

Since $\mathbf{3} \otimes \mathbf{3} = \mathbf{5} \oplus \mathbf{3} \oplus \mathbf{1}$ there is an essentially unique degree $(2,2)$ SU_2 invariant. This is k^2 and so $(k^2 p_O, k^2 q_O)$ spans an E inside the $2E$. Explicitly this is

$$
\begin{aligned}
p_1(z,\bar{z}) &= 2\sqrt{3}\left(z^4\bar{z}^2 + 2z^3\bar{z} + z^2\right), \\
q_1(z,\bar{z}) &= z^6\bar{z}^2 + 2z^5\bar{z} + z^4 + z^2\bar{z}^2 + 2z\bar{z} + 1.
\end{aligned} \tag{71}
$$

By calculating the projection matrix we can derive another pair of basis vectors in $2E$:

$$
\begin{aligned}
p_2(z,\bar{z}) &= \sqrt{3}\left(-z^6 + z^4\bar{z}^2 - 8z^3\bar{z} + z^2 - \bar{z}^2\right), \\
q_2(z,\bar{z}) &= -z^6\bar{z}^2 + 4z^5\bar{z} - 7z^4 - 7z^2\bar{z}^2 + 4z\bar{z} - 1,
\end{aligned} \tag{72}
$$

and the general invariant rational map has the same form as in the 3-Skyrmion case, (63). As before, $\phi = 0$ imposes the reflection symmetry of the true solution, and $\theta = 0$ corresponds to the holomorphic map.

In Fig. 4 we show $\mathcal{I}$ and $\mathcal{J}$ as a function of the angle θ. At $\theta = 0$ the graph of $\mathcal{J}$ has its global minimum. There is a local minimum at $\theta = \pm\pi/2$. The minimum value of $\mathcal{I}$ does not occur at the rational map value but at $\theta \approx -0.40$. Therefore, there is the possibility of deriving a lower energy. Indeed, minimizing the energy with respect to θ leads to $E = 1.127$ for $\theta \approx -0.138$. This energy is only 0.6% above the true solution. By contrast the holomorphic rational map ansatz energy is 1.5% above the true solution.

As before, we can examine the baryon density in the neighbourhood of a singularity of the holomorphic ansatz. In this case, the map is already oriented so that the holomorphic map has a singularity at $z = 0$. Setting $\theta = -0.138$ and expanding the density, B_R, in powers of z and $\bar{z}$ we obtain:

$$
B_R \approx 2.54 z\bar{z}. \tag{73}
$$

Therefore, B_R vanishes at $z = 0$, and there is no negative baryon density anywhere to lowest order.

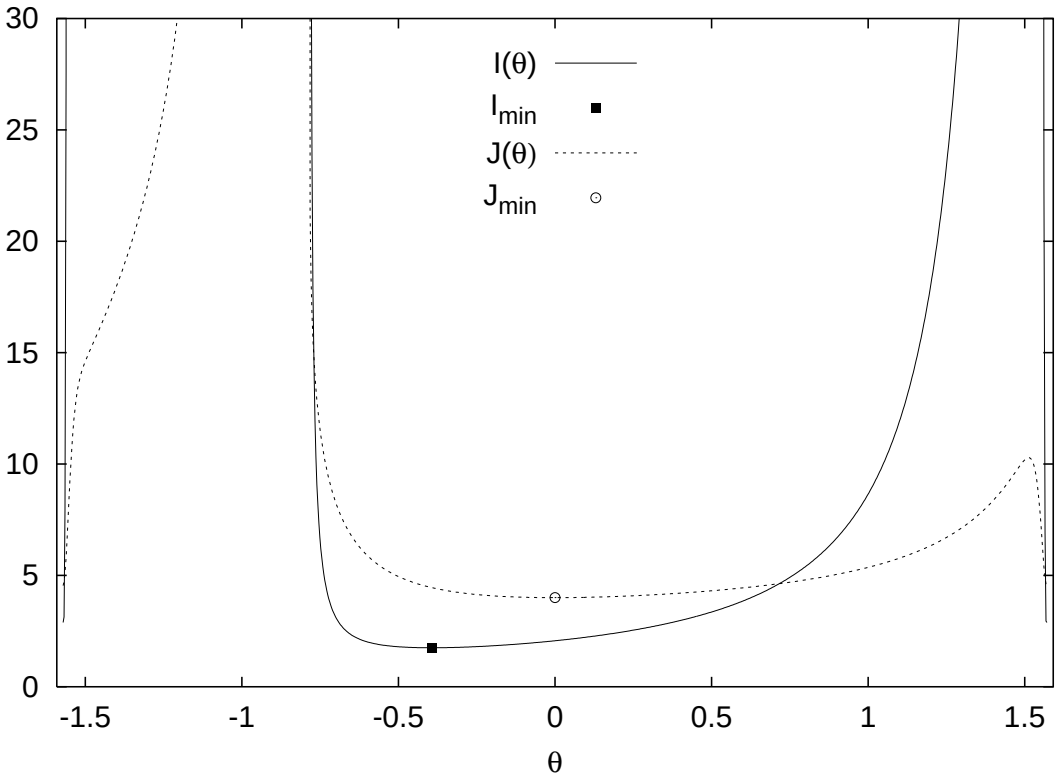

Figure 4: $\mathcal{I}$ and $\mathcal{J}$ as a function of θ for $B = 4$. Here $\mathcal{I}$ is rescaled by a factor of 10.

3.4 $B = 5^*$: the Octahedron

The $B = 5^*$ saddle point is octahedral in shape. The group theory involved in this example is very like the group theory required for $B = 3$. There is a holomorphic map

$$\begin{aligned} p_O(z) &= z^5 - 5z, \\ q_O(z) &= -5z^4 + 1, \end{aligned} \tag{74}$$

corresponding to the E_2' in

$$\mathbf{6}|_O = E_2' \oplus G'. \tag{75}$$

The generalization to $(6, 1)$ maps leads to a one-parameter family because

$$\begin{aligned} \mathbf{7} \otimes \mathbf{2} &= \mathbf{8} \oplus \mathbf{6}, \\ (\mathbf{8} \oplus \mathbf{6})|_O &= E_1' \oplus 2E_2' \oplus 2G'. \end{aligned} \tag{76}$$

Multiplying the holomorphic maps by the SU_2 invariant, $k = z\bar{z} + 1$, gives

$$\begin{aligned} p_1(z, \bar{z}) &= z^6\bar{z} + z^5 - 5z^2\bar{z} - 5z, \\ q_1(z, \bar{z}) &= -5z^5\bar{z} - 5z^4 + z\bar{z} + 1, \end{aligned} \tag{77}$$

and calculating the projection matrices gives

$$\begin{aligned} p_2(z, \bar{z}) &= 3z^6\bar{z} - 23z^5 - 15z^2\bar{z} + 11z, \\ q_2(z, \bar{z}) &= 11z^5\bar{z} - 15z^4 - 23z\bar{z} + 3. \end{aligned} \tag{78}$$

Thus, as before, a one-parameter family of invariant maps is given by (63) with $\phi = 0$. $\theta = 0$ gives the holomorphic map.

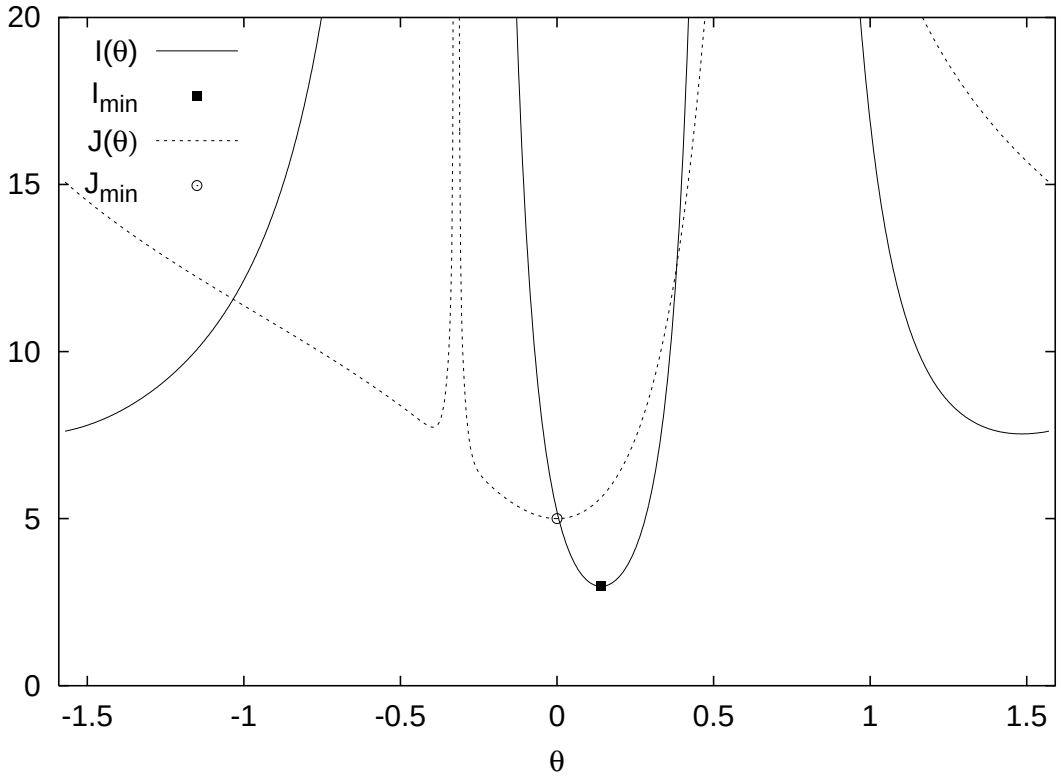

Figure 5: $\mathcal{I}$ and $\mathcal{J}$ as a function of θ for $B = 5^*$. Here $\mathcal{I}$ is rescaled by a factor of 10.

In Fig. 5 we display the graphs of $\mathcal{I}$ and $\mathcal{J}$ as a function of θ. There is a global minimum of $\mathcal{J}$ at the rational map value $\mathcal{J} = 5$. The graph of $\mathcal{I}$ has a minimum at $\theta \approx 0.141$. Minimizing the energy with respect to θ results in $E = 1.157$ for $\theta \approx 0.082$. This energy is only 1.7% above the true energy. In comparison, the energy of the holomorphic rational map ansatz is 8.3% above the true energy. This significant improvement gives an indication that negative baryon density plays an important role in this case. A local expansion shows that the non-holomorphic rational map has negative Jacobian determinant when z takes the values of the singularities of the holomorphic rational map. Finally, the integral of the negative baryon density is $B_- \approx 0.00097$ which is a factor of ten larger than for $B = 3$.

4 Conclusion

This paper was motivated by the theory of singularities of differentiable maps and, in particular, by Whitney's theorem. This theorem states that there are only three types of stable singularities of maps between three-manifolds. We showed that the holomorphic rational map ansatz for Skyrmions [9] does not have a stable singularity structure: it does not even allow folding. We introduced a non-holomorphic rational map ansatz that allows folding. For baryon numbers two, three and four, the approximate solutions derived from this ansatz are closer in energy to the true Skyrmions than any other ansatz solution.

The key idea of the non-holomorphic rational map ansatz is to construct maps between Riemann spheres which are not holomorphic but have the same symmetry as the true solutions. We described this construction in detail and calculated the non-holomorphic rational maps for baryon numbers two, three and four, and for the octahedrally-symmetric $B = 5^*$ saddle point. Non-holomorphic rational maps can have folding, and therefore, negative baryon density. We found that there is negative baryon density for $B = 3$ and $B = 5^*$ but not for $B = 2$ and $B = 4$.

By decomposing group representations we showed that there is a one-parameter family of tetrahedrally-symmetric $(4, 1)$ maps. These maps have topological degree three. The ansatz energy was minimized within this family to find the best approximation to the 3-Skyrmion. The $(4, 1)$ maps have anti-holomorphic degree one and so they are minimal generalizations of the original holomorphic map. For $B = 5^*$ the situation is similar: there is a one-parameter family of octahedrally symmetric $(6, 1)$ maps. However, for $B = 4$ the $(5, 1)$ maps do not contain a one-parameter family of octahedral maps, only the $(6, 2)$ maps do. The $(5, 1)$ maps can be thought of as the first order effect, and the $(6, 2)$ maps as a second order effect. In fact, for $B = 4$, the holomorphic rational map is remarkably close to the true solution. The energy error is 1.5%. The holomorphic rational map approximation to the 3-Skyrmion has an error of 3.3%. $B = 7$ seems to be similar to $B = 4$. The 7-Skyrmion is dodecahedral and it is easy to check that only the $(10, 3)$ maps contain a one-parameter family of icosahedrally-symmetric maps. Again, the holomorphic rational map is extremely close to the true solution, with an error of only 1.1%. Therefore, we do not expect that negative baryon density occurs for $B = 7$.

There is an icosahedrally-symmetric $B = 11^*$ saddle point. The holomorphic rational map ansatz approximates it quite poorly. It predicts an energy which is far larger than eleven 1-Skyrmions, whereas the true solution is a saddle-point solution with $E/B = 1.158$. This can be viewed as an indication that negative baryon density plays a major role. The representation theory also suggests that there is negative baryon density because there is a one-parameter family of icosahedrally symmetric $(12, 1)$ maps.

It seems possible to decide heuristically whether or not a Skyrmion of a certain symmetry possesses negative baryon density. In Sect. 1.3 we showed that a z^n singularity can be decomposed into folds which contain $n+1$ cusps and that there is a natural C_{n+1} symmetry which maps the cusps into each other. It seems likely that negative baryon density occurs if this C_{n+1} symmetry is compatible with the symmetry of the faces.

Direct computation shows that in the holomorphic rational map ansatz for $B = 2$, 3, 4, 5^*, 7 and 11^* all the singularities are of z^2 type. Therefore, negative baryon density occurs, if the faces have a C_3 symmetry. The faces of the tetrahedron, the octahedron and the icosahedron are equilateral triangles. This is consistent with what we found: there is negative baryon density for $B = 3$ and 5^*. It suggests that there is also negative baryon density for $B = 11^*$. On the other hand, the faces of a torus are round, the faces of a cube are squares and the faces of a dodecahedron are pentagons. Correspondingly, we did not find any negative baryon density for $B = 2$ and 4 and do not expect negative baryon density for $B = 7$.

In the 3-Skyrmion case we discussed the singularity structure at the origin. Assuming tetrahedral symmetry and generic singularities we conjectured a configuration with 16 folding surfaces, 30 cusp lines and 12 swallowtails. This is compatible with the instanton calculations in [18].

It appears that there is a large number of swallowtails, cusps and folds for both the

3-Skyrmion and $B = 5^*$ saddle point, but non-generic singularities for the 2-Skyrmion and 4-Skyrmion. Thus, while it may be that in non-extremal Skyrme configurations there are certain folding features associated with each interacting 1-Skyrmion, this is not necessarily apparent in the extremal configurations.

It might be interesting to examine the number of anti-vacuum points, that is, the number of points where $U = -1$. A 1-Skyrmion is centered around a single anti-vacuum point and in a configuration of well-separated Skyrmions, the individual Skyrmions can be thought of as being positioned at the anti-vacuum points. However, as the Skyrmions approach each other there may be more anti-vacuum points, some with positive Jacobian and some with negative. This is certainly what is implied by the folding seen in the 3-Skyrmion and $B = 5^*$ saddle point, and by the corresponding monopole configurations.

The topological charge of a BPS monopole is equal to the number of zeros of the Higgs field provided that the zeros are counted with their multiplicity. Furthermore, well-separated 1-monopoles are centered around a zero of the Higgs field. However, the total number of zeros can exceed the topological charge. In [29], 3-monopole fields were calculated using the mixture of analytic and numerical methods first described in [30, 16]. It was found that the number of zeros of the Higgs field can be as high as seven, with five zeros of positive winding number and two of negative winding number. In [17], the cubic 4-monopole, octahedral 5-monopole and dodecahedral 7-monopole calculated in [30, 16, 31] were examined and it was found that zeros with negative winding number occur for the octahedral 5-monopole but not for the cubic 4-monopole and the dodecahedral 7-monopole. This pattern is mimicked by what we have found for Skyrmions. This possibility was discussed in [17].

It is also interesting that in monopole dynamics, as an individual monopole approaches other monopoles, its zero of the Higgs field often splits into three zeros, two with positive winding and one with negative winding [29, 17]. Perhaps something similar happens in the case of Skyrmions.

Acknowledgments

We would like to thank N S Manton for useful discussion and for drawing our attention to the literature concerning the singularities of differentiable maps. One of us, S K thanks PPARC and the Studienstiftung des deutschen Volkes for financial assistance.

Appendix: Numerical Results

For convenience the main numerical results have been gathered together in Table 4. As discussed above, the table shows that the minima of $\mathcal{I}$ and $\mathcal{J}$ do not coincide and so the more general non-holomorphic rational map ansatz is closer to the true energy than the holomorphic ansatz. However, only for $B = 3$ and $B = 5^*$ are there regions of negative baryon density. These regions are quite small.

References

[1] T. H. R. Skyrme, *A nonlinear field theory*, Proc. Roy. Soc. Lond. **A260**: 127 (**1961**).

[2] P. M. Sutcliffe, *Skyrmions from kinks*, Phys. Lett. **B292**: 104 (**1992**).

	True	Holomorphic		Minimizing $\mathcal{I}$		Minimizing Energy			
B	E/B	$\mathcal{I}$	E/B	$\mathcal{I}$	B_-	$\mathcal{J}$	$\mathcal{I}$	B_-	E/B
1	1.2322	1	1.232	1	0	1	1	0	1.232
2	1.1791	5.81	1.208	4.20	0	2.04	4.98	0	1.191
3	1.1462	13.58	1.184	11.04	0.00088	3.04	11.48	0.00009	1.160
4	1.1201	20.65	1.137	17.50	0	4.04	18.95	0	1.127
5^*	1.138	52.10	1.232	29.72	0.00841	5.20	32.93	0.00097	1.157

True: These are the energies obtained in [7] by numerical minimization of the Skyrme energy.
Holomorphic: These are the values obtained in [9] using the holomorphic ansatz.
Minimizing $\mathcal{I}$: $\mathcal{I}$ is minimized within the class of maps considered.
Minimizing Energy: These are the best results obtained with the non-holomorphic rational map ansatz.

Table 4: The numerical results.

[3] V. B. Kopeliovich and B. E. Stern, *Exotic skyrmions*, JETP Lett. **45**: 203 (**1987**).

[4] J. J. M. Verbaarschot, *Axial symmetry of bound baryon number two solution of the Skyrme model*, Phys. Lett. **B195**: 235 (**1987**).

[5] E. Braaten, S. Townsend and L. Carson, *Novel structure of static multi-soliton solutions in the Skyrme model*, Phys. Lett. **B235**: 147 (**1990**).

[6] R. A. Battye and P. M. Sutcliffe, *Symmetric skyrmions*, Phys. Rev. Lett. **79**: 363 (**1997**), <hep-th/9702089>.

[7] R. A. Battye and P. M. Sutcliffe, *Solitonic fullerene structures in light atomic nuclei*, <hep-th/0012215>.

[8] S. Krusch, *S^3 skyrmions and the rational map ansatz*, Nonlinearity **13**: 2163 (**2000**), <hep-th/0006147>.

[9] C. J. Houghton, N. S. Manton and P. M. Sutcliffe, *Rational maps, monopoles and skyrmions*, Nucl. Phys. **B510**: 507 (**1998**), <hep-th/9705151>.

[10] N. S. Manton, *Geometry of skyrmions*, Commun. Math. Phys. **111**: 469 (**1987**).

[11] W. K. Baskerville and R. Michaels, *Classification of normal modes for multiskyrmions*, Phys. Lett. **B448**: 275 (**1999**), <hep-th/9802124>.

[12] M. Kugler, *Holes in the charge density of topological solitons*, In *Kingston 1997, Solitons* 93-97.

[13] C. L. Schat and N. N. Scoccola, *Multibaryons with heavy flavors in the Skyrme model*, Phys. Rev. **D61**: 034008 (**2000**), <hep-ph/9907271>.

[14] J. Hurtubise, *Monopoles and rational maps: A note on a theorem of Donaldson*, Commun. Math. Phys. **100**: 191 (**1985**).

[15] S. Jarvis, *A rational map for Euclidean monopoles via radial scattering*, J. Reine Angew. Math **524**: 17 (**2000**).

[16] C. J. Houghton and P. M. Sutcliffe, *Tetrahedral and cubic monopoles*, Commun. Math. Phys. **180**: 343–362 (**1996**), <hep-th/9601146>.

[17] P. M. Sutcliffe, *Monopole zeros*, Phys. Lett. **B376**: 103 (**1996**), <hep-th/9603065>.

[18] R. A. Leese and N. S. Manton, *Stable instanton generated Skyrme fields with baryon numbers three and four*, Nucl. Phys. **A572**: 575 (**1994**).

[19] M. F. Atiyah and N. S. Manton, *Skyrmions from instantons*, Phys. Lett. **B222**: 438 (**1989**).

[20] V. I. Arnold, S. M. Gusein-Zade and A. N. Varchenko, *Singularities of Differentiable Maps*, volume I, Birkhäuser (**1985**).

[21] B. Piette, P. M. Sutcliffe and W. J. Zakrzewski, *Soliton - anti-soliton scattering in (2+1)-dimensions*, Int. J. Mod. Phys. **C3**: 637–660 (**1992**).

[22] B. M. A. G. Piette, B. J. Schroers and W. J. Zakrzewski, *Dynamics of baby skyrmions*, Nucl. Phys. **B439**: 205–238 (**1995**), <hep-ph/9410256>.

[23] N. N. Scoccola and D. R. Bes, *Two-dimensional skyrmions on the sphere*, JHEP **09**: 012 (**1998**), <hep-th/9708146>.

[24] M. de Innocentis and R. S. Ward, *Skyrmions on the two-sphere*, <hep-th/0103046>.

[25] G. F. Koster, J. O. Dimmock, R. G. Wheeler and H. Statz, *Properties of the thirty-two point groups*, M.I.T. Press, Cambridge, Massachusetts (**1963**).

[26] J.-P. Serre, *Linear representations of finite groups*, Springer-Verlag, New York (**1993**).

[27] S. Krusch, *Structure of Skyrmions*, Ph.D. thesis, University of Cambridge (**2001**).

[28] W. H. Press, B. P. Flannery, S. A. Teukolsky and W. T. Vetterling, *Numerical Recipes*, Cambridge University Press (**1992**).

[29] C. J. Houghton and P. M. Sutcliffe, *Monopole scattering with a twist*, Nucl. Phys. **B464**: 59–84 (**1996**), <hep-th/9601148>.

[30] N. J. Hitchin, N. S. Manton and M. K. Murray, *Symmetric monopoles*, Nonlinearity **8**: 661 (**1995**).

[31] C. J. Houghton and P. M. Sutcliffe, *Octahedral and dodecahedral monopoles.*, Nonlinearity **9**: 385 (**1996**), <hep-th/9601147>.